Tonkie Khimicheskie Tekhnologii = Fine Chemical Technologies.
2024;19(6):547–554 ISSN 2686-7575 (Online)

UDC 621.762.2:681.5.013:549.76+546.763
https://doi.org/10.32362/2410-6593-2024-19-6-547-554
EDN WTSOXP

RESEARCH ARTICLE

Highly dispersed chromium(III) molybdate powders obtained by solid phase synthesis

Marina N. Miroshnichenko✉, Valery N. Kolosov

Tananaev Institute of Chemistry – Subdivision of the Federal Research Center "Kola Science Center of the Russian Academy of Sciences", Apatity, 184209 Russia

✉ *Corresponding author, e-mail: m.miroshnichenko@ksc.ru*

Abstract

Objectives. To obtain highly dispersed powders of chromium(III) molybdate $Cr_2(MoO_4)_3$ by solid phase synthesis and to study their porous structure.

Methods. After stirring in water, a mixture of Cr_2O_3 and MoO_3 oxide powders was dried in air and subjected to heat treatment in the temperature range of 600–800°C. After heat treatment, the products were identified by X-ray phase and sedimentation analysis. The specific surface area was measured using the Brunauer–Emmett–Teller static adsorption method. Porosity parameters were measured using the Barrett–Joyner–Halenda (BJH) method.

Results. The Gibbs free energy ΔG of the reaction between chromium and molybdenum oxides was calculated and it was shown that the process is characterized by a significant negative value of ΔG. Concurrently, the Gibbs energy exhibits a relatively weak dependence on temperature. The highly dispersed chromium(III) molybdate powders with specific surface area of 15.3–29.7 $m^2 \cdot g^{-1}$ obtained in this way were pure according to X-ray diffraction analysis. A study of the volume, diameter, and pore size distribution was conducted through the utilization of nitrogen adsorption–desorption isotherms in accordance with the BJH model.

Conclusions. It was demonstrated that $Cr_2(MoO_4)_3$ powders possess a mesoporous structure and are distinguished by a bimodal pore system comprising small pores with a diameter of 2–3 nm and larger pores with a diameter ranging from 15 to 30 nm.

Keywords

solid-phase synthesis, powder, oxide, chromium, molybdate, pores, specific surface area

Submitted: 11.09.2024
Revised: 18.09.2024
Accepted: 22.10.2024

For citation

Miroshnichenko M.N., Kolosov V.N. Highly dispersed chromium(III) molybdate powders obtained by solid phase synthesis. *Tonk. Khim. Tekhnol. = Fine Chem. Technol*. 2024;19(6):547–554. https://doi.org/10.32362/2410-6593-2024-19-6-547-554

НАУЧНАЯ СТАТЬЯ

Высокодисперсные порошки молибдата хрома(III), полученные твердофазным синтезом

М.Н. Мирошниченко✉, В.Н. Колосов

Институт химии и технологии редких элементов и минерального сырья им. И.В.Тананаева – обособленное подразделение Федерального государственного бюджетного учреждения науки Федерального исследовательского центра «Кольский научный центр Российской академии наук», Апатиты, 184209 Россия

✉ *Автор для переписки, e-mail: m.miroshnichenko@ksc.ru*

Аннотация

Цели. Получить высокодисперсные порошки молибдата хрома(III) $Cr_2(MoO_4)_3$твердофазным синтезом и исследовать их пористую структуру.

Методы. Смесь порошков оксидов Cr_2O_3 и MoO_3 после перемешивания в воде просушивали на воздухе и подвергали термообработке в температурном интервале 600–800°C. После термообработки продукты идентифицировали методами рентгенофазового и седиментационного анализа. Величину удельной поверхности измеряли адсорбционным статическим методом Брунауэра–Эммета–Теллера, а параметры пористости — методом Баррета–Джойнера–Халенды (BJH, Barrett–Joyner–Halenda).

Результаты. Рассчитана свободная энергия Гиббса ΔG реакции между оксидами хрома(III) и молибдена(VI). Показано, что процесс характеризуется значительной отрицательной величиной ΔG. При этом энергия Гиббса слабо зависит от температуры. Получены чистые по данным рентгеновского анализа высокодисперсные порошки молибдата хрома(III) с удельной поверхностью 15.3–29.7 $м^2 \cdot г^{-1}$. С использованием изотерм адсорбции–десорбции азота при помощи модели BJH исследованы объем, диаметр и распределение пор по размерам.

Выводы. Показано, что порошки $Cr_2(MoO_4)_3$ имеют мезопористую структуру и характеризуются бимодальной системой пор, состоящей из небольших пор с размерами 2–3 нм и более крупных пор с размерами от 15 до 30 нм.

Ключевые слова

твердофазный синтез, порошок, оксид, хром, молибдат, поры, удельная поверхность

Поступила: 11.09.2024
Доработана: 18.09.2024
Принята в печать: 22.10.2024

Для цитирования

Мирошниченко М.Н., Колосов В.Н. Высокодисперсные порошки молибдата хрома(III), полученные твердофазным синтезом. *Тонкие химические технологии*. 2024;19(6):547–554. https://doi.org/10.32362/2410-6593-2024-19-6-547-554

INTRODUCTION

Chromium(III) molybdenum $Cr_2(MoO_4)_3$ belongs to the family of chemical compounds with the general formula $A_2M_3O_{12}$, where A is a trivalent transition metal or lanthanide, and M is molybdenum or tungsten [1–6]. These compounds possess distinctive structural, thermal, magnetic, and electrical characteristics. These materials are distinguished by a phase transition from a low-temperature monoclinic structure ($P2_1/a$) to a high-temperature orthorhombic structure ($Pbcn$). Both structures are microporous, forming open interstitial cationless frameworks consisting of AO_6 octahedra and MO_4 tetrahedra connected by vertices. The AO_6 octahedra are connected to the MO_4 tetrahedra by a common oxygen atom at each vertex. In orthorhombic modification, compounds $A_2M_3O_{12}$ exhibit negative thermal expansion, the causes of which have not yet been precisely determined [7]. Materials exhibiting negative thermal expansion have significant potential for use in the creation of composite materials with an adjustable coefficient of thermal expansion [8]. Based on the compounds $A_2M_3O_{12}$, functional materials can be created for various purposes. In particular, chromium(III) molybdate is a ferrimagnet [9] and is characterized by two different conduction mechanisms [10]. Below the structural phase transition temperature (about 650 K) $Cr_2(MoO_4)_3$ is a *p*-type semiconductor, while above it is an *n*-type semiconductor. Additionally, chromium(III) molybdate displays catalytic activity and can be employed as a catalyst in alcohol oxidation, *n*-octane dehydrogenation, and other chemical reactions [11–14].

In order to obtain $Cr_2(MoO_4)_3$, the following are used: mechanosynthesis [15, 16]; solid-phase synthesis [17]; sol–gel method [9], co-precipitation of a soluble chromium salt and molybdenum acid [18]; and co-decomposition of a mixture of bichromate and ammonium paramolybdate

followed by calcination of the resulting product [19]. The techniques currently available possess certain disadvantages. These include the length of time required for the process, the necessity for maintaining a constant pH value of the reagent solutions, and the occurrence of hydrolytic processes in the solutions themselves. Furthermore, the resulting chromium(III) molybdenum powders exhibit an inadequate specific surface area. For example, the surface of powders obtained using mechanosynthesis is 1.3–3.6 $m^2 \cdot g^{-1}$ [15].

The objective of this study is to synthesize highly dispersed chromium(III) molybdate powders by means of a solid-phase approach with a view to investigating their porous structure.

MATERIALS AND METHODS

Oxides of MoO_3 (pure, TU 6-094471-77, *Khimreaktivnab*, Russia) and Cr_2O_3 were used as precursors. Chromium(III) oxide was obtained by calcination of ammonium dichromate $(NH_4)_2Cr_2O_7$ (chemically pure, GOST 3763-76[1], *Khimreaktivnab)*. Cr_2O_3 and MoO_3 oxide powders were weighed in accordance with the stoichiometric ratio of chromium and molybdenum in the compound $Cr_2(MoO_4)_3$. The oxides were then mixed in water in a solid/liquid phase ratio = 1 : 5 using an overhead stirrer RW16basic (*IKA*, Germany) for 3 h. The rotation speed of the mixer is 320 min^{-1}. Following the mixing process, the mixture was subjected to drying in air at a temperature range of 80–85°C. Subsequently the mixture underwent heat treatment in a laboratory-based muffle furnace (*Sikron*, Russia) at an initial temperature of 600°C for a period of 5 h. This was followed by a repeated heat treatment in the range of 700–800°C for a further 6 h.

Phase analysis of the reagents and the products obtained was determined using a *Shimadzu* XRD-6000 diffractometer (Japan) (CuK_α-radiation) using the ICCD PDF-2 diffractometric database[2]. The average particle size D of $Cr_2(MoO_4)_3$ powder was estimated under the assumption that they have a spherical shape, according to the formula:

$$D = \frac{6}{S_{BET} \cdot \rho}, \quad (1)$$

wherein S_{BET} is the specific surface area of the powder, ρ is the density of $Cr_2(MoO_4)_3$. The specific surface area was measured by means of the Brunauer–Emmett–Teller (BET) adsorption static method. The porosity parameters were measured by the Barrett–Joyner–Halenda method on a Micrometrics TriStar II 3020 device (*Micrometrics Instrument Corporation*, USA) using nitrogen adsorption–desorption isotherms. The particle size distribution of the powders was analyzed on a photometric sedimentometer FSH-6K (*Labnauchpribor*, Russia).

RESULTS AND DISCUSSION

The synthesis of chromium(III) molybdate is based on a solid phase reaction between oxides of the corresponding metals:

$$Cr_2O_3\,(solid) + 3MoO_3\,(solid) = Cr_2(MoO_4)_3\,(solid) \quad (2)$$

The Gibbs free energy ΔG of the reaction (2) was calculated as a function of temperature (Fig. 1).

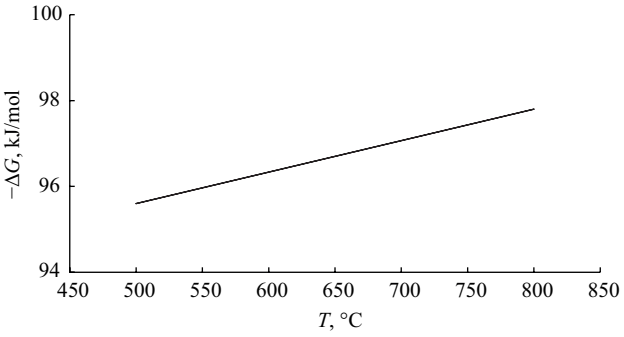

Fig. 1. Gibbs free energy ΔG as a function of the reaction temperature for the formation of chromium(III) molybdate

The calculation was carried out using the entropy method, while considering the aggregate state of the reaction participants. The necessary thermodynamic values of chromium oxides and molybdenum used in the calculations were taken from [20, 21]. The reaction (2) is energetically advantageous for synthesis within the specified temperature range. In this case, the Gibbs energy is observed to exhibit a relatively weak dependence on temperature. The chromium(III) molybdate powders, which were found to be of a high degree of purity according to X-ray phase analysis, were obtained as a result of double sintering of the charge. The initial charge and reaction products are displayed in Fig. 2, together with their respective diffractograms, subjected to heat treatment.

The research yielded chromium(III) molybdate powders with a specific surface area of 15.3–29.6 $m^2 \cdot g^{-1}$. Figure 3 illustrates the typical integral particle size distribution observed in powder samples.

[1] GOST 3763-76. State Standard of the USSR. Reagents. Ammonium bichromate. Specifications. Moscow: IPK Izdatelstvo Standartov; 1998.

[2] https://www.icdd.com/pdf-2/. Accessed November 22, 2022.

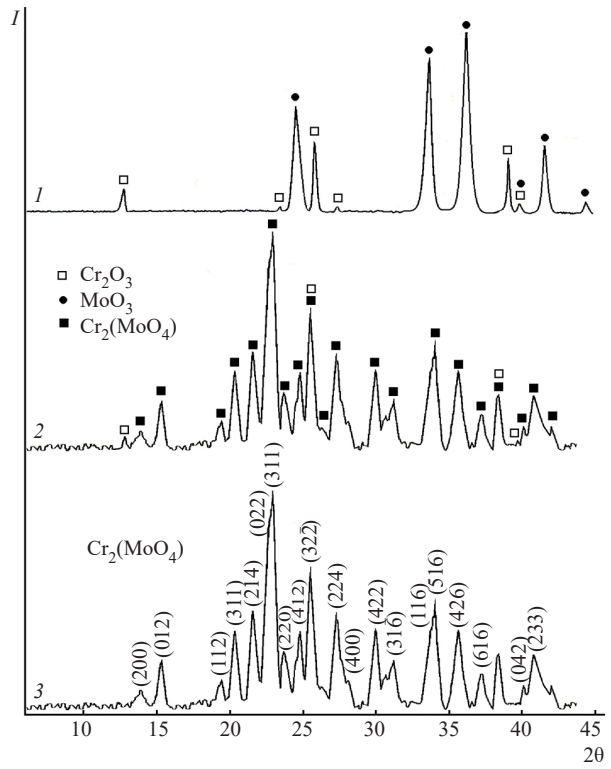

Fig. 2. Initial mixture of metal oxides (*1*) and the resulting diffractogram after heat treatment (*2*, *3*). Sintering conditions: (*2*) 600°C, 5 h + 800°C, 4 h; (*3*) 600°C, 5 h + 800°C, 6 h

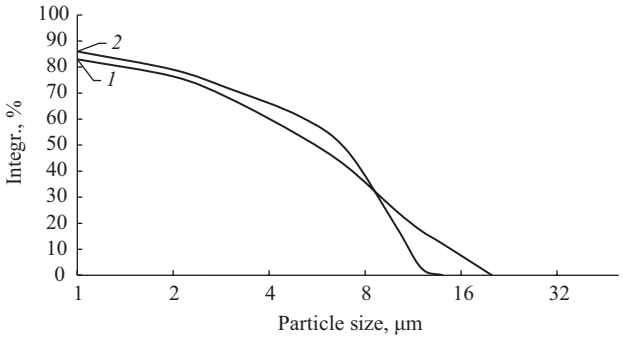

Fig. 3. Integral particle size distribution of $Cr_2(MoO_4)_3$ powders. Specific surface area of powders: (*1*) 15.3 $m^2 \cdot g^{-1}$, (*2*) 29.7 $m^2 \cdot g^{-1}$

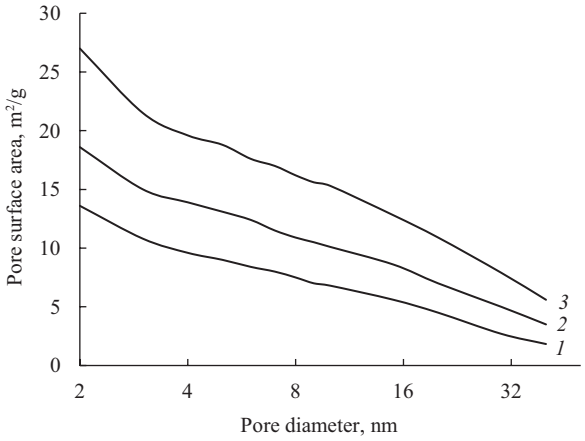

Fig. 4. Dependencies of the total pore surface on their average diameter for $Cr_2(MoO_4)_3$ powders. Specific surface area of powders: (*1*) 15.3, (*2*) 20.3, (*3*) 29.7 $m^2 \cdot g^{-1}$

Figure 3 illustrates that, despite the considerable discrepancy in the value of specific surface area, the powder samples exhibit minimal variation in their particle size distribution. The majority of particles, comprising approximately 70% of the total, are smaller than 9 μm, with a further 25% less than 2 μm in size. According to calculations using formula (1), the average particle size of $Cr_2(MoO_4)_3$ is in the range of 60–115 nm. It can thus be surmised that, in view of the specific surface area of the powders, the particles of the chromium molybdenum powder are to a considerable extent agglomerated. The process of agglomeration results in the formation of a porous material.

Figure 4 illustrates the relationship between the total surface area of the pores and their average diameter.

The total surface area of the powders obtained is approximately equivalent to the total surface area of the pores. Therefore, the outer surface area of the chromium(III) molybdate particles is insignificant in comparison to the developed inner porous surface area, which constitutes the majority of the powder's surface area. The type of adsorption–desorption isotherms of $Cr_2(MoO_4)_3$ powders is shown in Fig. 5. The isotherms observed for the powders can be classified as type IV according to the IUPAC classification, with the presence of H3 hysteresis loops. Isotherms of this nature are typical of mesoporous substances, characterized by disordered aggregates forming slit-shaped pores [22, 23]. With an increase in the specific surface area of powders from 15.3 to 29.6 $m^2 \cdot g^{-1}$, the adsorption–desorption isotherms show an increase in the amount of adsorbed nitrogen (Fig. 5). This is a consequence of the increased porosity of the material, which allows for greater permeability.

As illustrated in Fig. 6, the pore size distribution of chromium(III) molybdenum powders exhibits a bimodal character in the mesoporous region. The subject of such materials is currently attracting a growing amount of attention. When employed in the context of catalysts, these materials have been demonstrated to effectively reduce the diffusion resistance and enhance the catalytic efficiency of heterogeneous reactions [24–26].

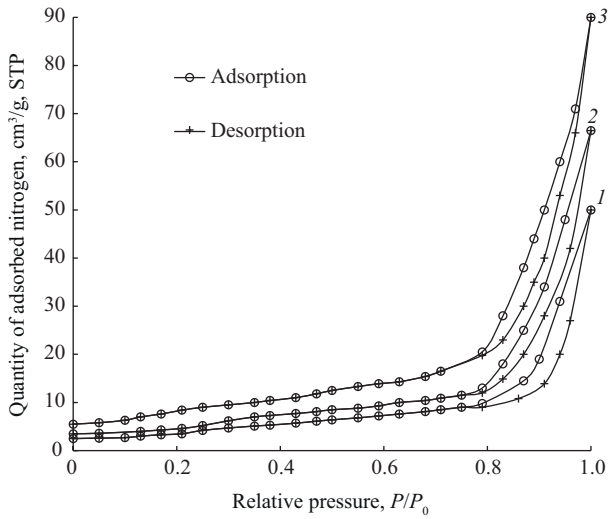

Fig. 5. Nitrogen adsorption–desorption isotherms of $Cr_2(MoO_4)_3$ powders
(STP is the standard temperature of 273.15 K (0°C, 32°F) and pressure of exactly 105 Pa (1 atm, 1 bar)).
Specific surface area of powders:
(*1*) 15.3,
(*2*) 20.3,
(*3*) 29.7 $m^2 \cdot g^{-1}$

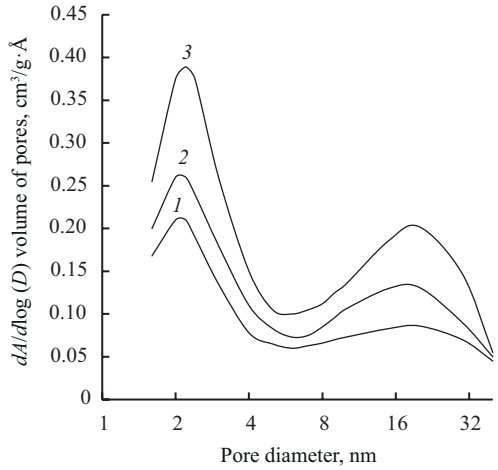

Fig. 6. Pore distribution in $Cr_2(MoO_4)_3$ powders.
Specific surface area of powders:
(*1*) 15.3,
(*2*) 20.3,
(*3*) 29.7 $m^2 \cdot g^{-1}$

According to [27], the bimodal pore distribution is due to the presence of solid aggregates in powders, in which there are two types of pores. One category of pores is of a smaller intra-aggregate size, while the other is of a larger inter-aggregate size. In accordance with this definition, the intraaggregate pores of the obtained chromium(III) molybdate powders have a diameter of 2–3 nm, while the interaggregate pores exhibit a broader distribution, with a diameter ranging from 15 to 30 nm. Modifying the heat treatment parameters of the initial metal oxide mixture allows for the alteration of the pore density within the resulting powder. With an increase in the specific surface area of chromium(III) molybdate powders, the pore volume of both pore types increases (Fig. 6).

CONCLUSIONS

A solid-phase method was employed at temperatures between 600 and 800°C to synthesize chromium(III) molybdenum powders with a high degree of dispersion and a specific surface area of 15.3 to 29.7 $m^2 \cdot g^{-1}$, as determined by X-ray analysis. The pore distribution of powders is bimodal in nature. Intraaggregate pores are 2–3 nm, while interaggregate pores are at the level of 15–30 nm. The resulting powders can be used as precursors in the creation of catalysts.

Authors' contributions

M.N. Miroshnichenko—synthesis of compounds, writing the text of the article.

V.N. Kolosov—processing experimental results, writing the text of the article.

The authors declare no conflicts of interest.

REFERENCES

1. Tyagi A.K., Achary S.N., Mathews M.D. Phase Transition and Negative Thermal Expansion in $A_2(MoO_4)_3$ System (A=Fe^{3+}, Cr^{3+} and Al^{3+}). *J. Alloys Compd*. 2002;339(1–2):1377–1383. https://doi.org/10.1016/S0925-8388(01)02003-5
2. Liu J., Sharma N. Thermal Evolution and Phase Transitions in Electrochemically Activated $Sc_2(MoO_4)_3$. *Inorg. Chem.* 2019;58(9):9964–9973. https://doi.org/10.1021/acs.inorgchem.9b01116
3. Pudge G.J.F., Hutchings G.J., Kondrat S.A., Morrison K., Perkins E.F., Rushbya A.V., Bartley J.K. Iron molybdate catalysts synthesised via dicarboxylate decomposition for the partial oxidation of methanol to formaldehyde. *Catal. Sci. Technol.* 2022;12(14):4552–4560. http://doi.org/10.1039/D2CY00699E
4. Dias A.P.S., Rijo B., Kiennemann A., Portela M.F. Methanol oxidation over iron molybdate catalysts. Main and side reactions kinetics. *Appl. Catal. A Gen*. 2023;658(5):119118. https://doi.org/10.1016/j.apcata.2023.119118
5. Gurusamy L., Karuppasamy L., Anandan S., Liu C.-H., Wu J.J. Recent advances on metal molybdate-based electrode materials for supercapacitor application. *J. Energy Storage*. 2024;79(2):110122. https://doi.org/10.1016/j.est.2023.110122
6. El-Aryan Y.F., Melhi S. Adsorption Study of Eriochrome Black T Dye on Polyacrylonitrile Chromium molybdate Composite. *Russ. J. Appl. Chem*. 2024. https://doi.org/10.1134/S1070427224020125
7. Miller W., Smith C.W., Mackenzie D.S., Evans K.E. Negative thermal expansion: a review. *J. Mater. Sci.* 2009;44(20):5441–5451. https://doi.org/10.1007/s10853-009-3692-4
8. Zhang Z., Sun W., Zheng Q., Liu H., Zhou M., Wang W., Chen X. Tuning the Phase Transition Temperature of $Cr_2(MoO_4)_3$ by A-site Substitution of Scandium. *Ceram. Int.* 2018;44(18):22165–22171. https://doi.org/10.1016/j.ceramint.2018.08.329
9. Battle P.D., Cheetham A.K., Harrison W.T.A., Pollard N.J., Faber J. The Structure and Magnetic Properties of Chromium(III) Molybdate. *J. Solid State. Chem*. 1985;58(2):221–225. https://doi.org/10.1016/0022-4596(85)90238-5
10. Ansari T.H., Yadava Y.P. Electrical Conduction in Polycrystalline Chromium Molybdate. *Mater. Lett.* 1990;9(11):469–473. https://doi.org/10.1016/0167-577x(90)90120-b
11. Popov T.S., Popov B.I., Bibin V.N., Bliznakov G.M., Boreskov G.K. Catalytic Properties of Chromium-Molybdenum Oxide Catalysts in Methanol Oxidation. React. *Kinet. Catal. Lett*. 1975;3(2):169–175. https://doi.org/10.1007/bf02187510
12. Oudghiri-Hassani H. Synthesis, Characterization and Application of Chromium Molybdate for Oxidation of Methylene Blue Dye. *J. Mater. Environ. Sci.* 2018;9(2):1051–1057. https://doi.org/10.26872/jmes.2018.9.3,117
13. Yadagiri M., Ramakrishna S., Ravi G., Suresh P., Sreenu K., Jaya-Prakash D., Vithal M. Preparation, Characterization and Photocatalytic Studies of $Cr_2(MoO_4)_3$ and Nitrogen-Doped $Cr_2(MoO_4)_3$. *Chem. Chem. Technol*. 2015;9(4):391–399. https://doi.org/10.23939/chcht09.04.391
14. Bandaru H., Mahomed A.S., Singh S., Friedrich H.B. The Effect of Varying the Metal Ratio in a Chromium Molybdate Catalysts for the Oxidative Dehydrogenation of *n*-octane. *Mol. Catal.* 2018;460(9):74–82. https://doi.org/10.1016/j.mcat.2018.09.017
15. Klissurski D., Mancheva M., Iordanova R., Kunev B. Synthesis of $Cr_2(MoO_4)_3$ from Mechanically Activated Precursors. *Khimiya v interesakh ustoichivogo razvitiya = Chemistry for Sustainable Development*. 2005;13(2):229–232(in Russ.).

СПИСОК ЛИТЕРАТУРЫ

1. Tyagi A.K., Achary S.N., Mathews M.D. Phase Transition and Negative Thermal Expansion in $A_2(MoO_4)_3$ System (A=Fe^{3+}, Cr^{3+} and Al^{3+}). *J. Alloys Compd*. 2002;339(1–2):1377–1383. https://doi.org/10.1016/S0925-8388(01)02003-5
2. Liu J., Sharma N. Thermal Evolution and Phase Transitions in Electrochemically Activated $Sc_2(MoO_4)_3$. *Inorg. Chem.* 2019;58(9):9964–9973. https://doi.org/10.1021/acs.inorgchem.9b01116
3. Pudge G.J.F., Hutchings G.J., Kondrat S.A., Morrison K., Perkins E.F., Rushbya A.V., Bartley J.K. Iron molybdate catalysts synthesised via dicarboxylate decomposition for the partial oxidation of methanol to formaldehyde. *Catal. Sci. Technol*. 2022;12(14):4552–4560. http://doi.org/10.1039/D2CY00699E
4. Dias A.P.S., Rijo B., Kiennemann A., Portela M.F. Methanol oxidation over iron molybdate catalysts. Main and side reactions kinetics. *Appl. Catal. A Gen*. 2023;658(5):119118. https://doi.org/10.1016/j.apcata.2023.119118
5. Gurusamy L., Karuppasamy L., Anandan S., Liu C.-H., Wu J.J. Recent advances on metal molybdate-based electrode materials for supercapacitor application. *J. Energy Storage*. 2024;79(2):110122. https://doi.org/10.1016/j.est.2023.110122
6. El-Aryan Y.F., Melhi S. Adsorption Study of Eriochrome Black T Dye on Polyacrylonitrile Chromium molybdate Composite. *Russ. J. Appl. Chem*. 2024. https://doi.org/10.1134/S1070427224020125
7. Miller W., Smith C.W., Mackenzie D.S., Evans K.E. Negative thermal expansion: a review. *J. Mater. Sci.* 2009;44(20):5441–5451. https://doi.org/10.1007/s10853-009-3692-4
8. Zhang Z., Sun W., Zheng Q., Liu H., Zhou M., Wang W., Chen X. Tuning the Phase Transition Temperature of $Cr_2(MoO_4)_3$ by A-site Substitution of Scandium. *Ceram. Int.* 2018;44(18):22165–22171. https://doi.org/10.1016/j.ceramint.2018.08.329
9. Battle P.D., Cheetham A.K., Harrison W.T.A., Pollard N.J., Faber J. The Structure and Magnetic Properties of Chromium(III) Molybdate. *J. Solid State. Chem*. 1985;58(2):221–225. https://doi.org/10.1016/0022-4596(85)90238-5
10. Ansari T.H., Yadava Y.P. Electrical Conduction in Polycrystalline Chromium Molybdate. *Mater. Lett.* 1990;9(11):469–473. https://doi.org/10.1016/0167-577x(90)90120-b
11. Popov T.S., Popov B.I., Bibin V.N., Bliznakov G.M., Boreskov G.K. Catalytic Properties of Chromium-Molybdenum Oxide Catalysts in Methanol Oxidation. React. *Kinet. Catal. Lett*. 1975;3(2):169–175. https://doi.org/10.1007/bf02187510
12. Oudghiri-Hassani H. Synthesis, Characterization and Application of Chromium Molybdate for Oxidation of Methylene Blue Dye. *J. Mater. Environ. Sci.* 2018;9(2):1051–1057. https://doi.org/10.26872/jmes.2018.9.3,117
13. Yadagiri M., Ramakrishna S., Ravi G., Suresh P., Sreenu K., Jaya-Prakash D., Vithal M. Preparation, Characterization and Photocatalytic Studies of $Cr_2(MoO_4)_3$ and Nitrogen-Doped $Cr_2(MoO_4)_3$. *Chem. Chem. Technol*. 2015;9(4):391–399. https://doi.org/10.23939/chcht09.04.391
14. Bandaru H., Mahomed A.S., Singh S., Friedrich H.B. The Effect of Varying the Metal Ratio in a Chromium Molybdate Catalysts for the Oxidative Dehydrogenation of *n*-octane. *Mol. Catal.* 2018;460(9):74–82. https://doi.org/10.1016/j.mcat.2018.09.017
15. Klissurski D., Mancheva M., Iordanova R., Kunev B. Synthesis of $Cr_2(MoO_4)_3$ from Mechanically Activated Precursors. *Химия в интересах устойчивого развития.* 2005;13(2):229–232.

16. Batanov A.A., Rumyantsev R.N., Goryanskaya V.A., Il'in A.A., Il'in A.P. Mechanochemical synthesis of chromium(III) molybdates on the basis of various precursors. *Vestnik Tverskogo Gosudarstvennogo Universiteta. Seriya: Khimiya = Herald of Tver State University. Series: Chemistry*. 2020;1(39):96–109 (in Russ.). https://doi.org/10.26456/vtchem2020.1.11
17. Shurdumov G.K., Tlikhuryaeva M.M., Kardanova Yu.L., Shurdumov B.K. Solid-phase synthesis of highly dispersed chromium(III) molybdate based on the Cr_2SO_4-Na_2CO_3-MoO_3 system. *Khimiya v interesakh ustoichivogo razvitiya = Chemistry for Sustainable Development*. 2016;24:805–810 (in Russ.). https://doi.org/10.15372/KhUR20160611
18. Plyasova L.M., Kefeli L.M. X-ray study of chromium and aluminum molybdates. *Izvestiya AN SSSR. Neorganicheskie Materialy*. 1967;3(5):906–908 (in Russ.).
19. Butukhanov V.D., Get'man E.I., Mokhosoev M.V. Interaction of lithium molybdate with chromium molybdate. *Zhurnal Neorganicheskoi Khimii.* 1972;17(4):1169–1171 (in Russ.).
20. Binnewies M., Mike E. *Thermochemical Data of Elements and Compounds*. Wenham: Wiley-VCH Verlag GmbH; 2002. 936 p. https://doi.org/10.1002/9783527618347
21. Tamm M.E., Tretyakov Yu.D. *Neorganicheskaya khimiya* (*Inorganic Chemistry*): in 3 v. Moscow: Akademiya; 2004. V.1. 240 p. (in Russ.).
22. Sing K.S.W. Reporting Physisorption Data for Gas/Solid Systems with Special Reference to the Determination of Surface Area and Porosity (Recommendations 1984). *Pure Appl. Chem*. 1985;57(4):603–619. https://doi.org/10.1351/pac198557040603
23. Thommes M., Kaneko K., Neimark A.V., Olivier J.P., Rodriguez-Reinoso F., Rouquerol J., Sing K.S.W. Physisorption of Gases, with Special Reference to the Evaluation of Surface Area and Pore Size Distribution (IUPAC Technical Report). *Pure Appl. Chem*. 2015;87(9):1051–1069. https://doi.org/10.1515/pac-2014-1117
24. Yu J., Wang G., Cheng B., Zhou M. Effects of Hydrothermal Temperature and Time on the Photocatalytic Activity and Microstructures of Bimodal Mesoporous TiO_2 Powders. *Appl. Catal. B: Environmental*. 2007;69(3–4):171–180. https://doi.org/10.1016/j.apcatb.2006.06.022
25. Yang L., Guo M., Zhang F., Jing Y., Wang Y., Luo G. Controllable Preparation of γ-Alumina Nanoparticles with Bimodal Pore Size Distribution in Membrane Dispersion Microreactor. *Particuology*. 2018;41(12):1–10. https://doi.org/10.1016/j.partic.2018.04.001
26. Fuentes-Quezada E., de la Llave E., Halac E., Jobbágy M., Viva F.A., Bruno M.M., Corti H.R. Bimodal Mesoporous Hard Carbons from Stabilized Resorcinol-Formaldehyde Resin and Silica Template with Enhanced Adsorption Capacity. *Chem. Eng. J.* 2019;360(3):631–644. https://doi.org/10.1016/j.cej.2018.11.235
27. Kumar K.-N.P., Kumar J., Keizer K. Effect of Peptization on Densification and Phase-Transformation Behavior of Sol–Gel-Derived Nanostructured Titania. *J. Am. Ceram. Soc*. 1994;77(5):1396–1400. https://doi.org/10.1111/j.1151-2916.1994.tb05426.x

16. Батанов А.А., Румянцев Р.Н., Горянская В.А., Ильин А.А., Ильин А.П. Механохимический синтез молибдатов хрома(III) на основе различных прекурсоров. *Вестник ТвГУ. Серия: Химия*. 2020;1(39):96–109. https://doi.org/10.26456/vtchem2020.1.11
17. Шурдумов Г.К., Тлихуряева М.М., Карданова Ю.Л., Шурдумов Б.К. Твердофазный синтез высокодисперсного молибдата хрома(III) на основе системы Cr_2SO_4-Na_2CO_3-MoO_3. *Химия в интересах устойчивого развития*. 2016;24:805–810. https://doi.org/10.15372/KhUR20160611
18. Плясова Л.М., Кефели Л.М. Рентгенографическое исследование молибдатов хрома и алюминия. *Изв. АН СССР. Неорган. материалы*. 1967;3(5):906–908.
19. Бутуханов В.Д., Гетьман Е.И., Мохосоев М.В. Взаимодействие молибдата лития с молибдатом хрома. *Журн. неорган. химии*. 1972;17(4):1169–1171.
20. Binnewies M., Mike E. *Thermochemical Data of Elements and Compounds*. Wenham: Wiley-VCH Verlag GmbH; 2002. 936 p. https://doi.org/10.1002/9783527618347
21. Тамм М.Е., Третьяков Ю.Д. *Неорганическая химия*: в 3 т. М.: Академия; 2004. Т.1. 240 с.
22. Sing K.S.W. Reporting Physisorption Data for Gas/Solid Systems with Special Reference to the Determination of Surface Area and Porosity (Recommendations 1984). *Pure Appl. Chem*. 1985;57(4):603–619. https://doi.org/10.1351/pac198557040603
23. Thommes M., Kaneko K., Neimark A.V., Olivier J.P., Rodriguez-Reinoso F., Rouquerol J., Sing K.S.W. Physisorption of Gases, with Special Reference to the Evaluation of Surface Area and Pore Size Distribution (IUPAC Technical Report). *Pure Appl. Chem*. 2015;87(9):1051–1069. https://doi.org/10.1515/pac-2014-1117
24. Yu J., Wang G., Cheng B., Zhou M. Effects of Hydrothermal Temperature and Time on the Photocatalytic Activity and Microstructures of Bimodal Mesoporous TiO_2 Powders. *Appl. Catal. B: Environmental*. 2007;69(3–4):171–180. https://doi.org/10.1016/j.apcatb.2006.06.022
25. Yang L., Guo M., Zhang F., Jing Y., Wang Y., Luo G. Controllable Preparation of γ-Alumina Nanoparticles with Bimodal Pore Size Distribution in Membrane Dispersion Microreactor. *Particuology*. 2018;41(12):1–10. https://doi.org/10.1016/j.partic.2018.04.001
26. Fuentes-Quezada E., de la Llave E., Halac E., Jobbágy M., Viva F.A., Bruno M.M., Corti H.R. Bimodal Mesoporous Hard Carbons from Stabilized Resorcinol-Formaldehyde Resin and Silica Template with Enhanced Adsorption Capacity. *Chem. Eng. J.* 2019;360(3):631–644. https://doi.org/10.1016/j.cej.2018.11.235
27. Kumar K.-N.P., Kumar J., Keizer K. Effect of Peptization on Densification and Phase-Transformation Behavior of Sol–Gel-Derived Nanostructured Titania. *J. Am. Ceram. Soc*. 1994;77(5):1396–1400. https://doi.org/10.1111/j.1151-2916.1994.tb05426.x

About the authors

Marina N. Miroshnichenko, Cand. Sci. (Eng.), Researcher, Tananaev Institute of Chemistry — Subdivision of the Federal Research Center "Kola Science Center of the Russian Academy of Sciences" (ICT KSC RAS) (26a, Akademgorodok, Apatity, Murmansk oblast, 184209, Russia). E-mail: m.miroshnichenko@ksc.ru. ResearcherID P-9964-2017, Scopus Author ID 8522192100, RSCI SPIN-code 7948-2708, https://orcid.org/0000-0002-5925-4561

Valery N. Kolosov, Dr. Sci. (Eng.), Chief Researcher, Tananaev Institute of Chemistry — Subdivision of the Federal Research Center "Kola Science Center of the Russian Academy of Sciences" (ICT KSC RAS) (26a, Akademgorodok, Apatity, Murmansk oblast, 184209, Russia). E-mail: v.kolosov@ksc.ru. ResearcherID Q-8446-2017, Scopus Author ID 35275498200, RSCI SPIN-code 1801-2839, https://orcid.org/0000-0002-4749-236X

Об авторах

Мирошниченко Марина Николаевна, к.т.н., научный сотрудник, Институт химии и технологии редких элементов и минерального сырья им. И.В.Тананаева – обособленное подразделение Федерального государственного бюджетного учреждения науки Федерального исследовательского центра «Кольский научный центр Российской академии наук» (ИХТРЭМС КНЦ РАН) (184209, Россия, г. Апатиты, Мурманская обл., Академгородок, д. 26а). E-mail: m.miroshnichenko@ksc.ru. ResearcherID P-9964-2017, Scopus Author ID 8522192100, SPIN-код РИНЦ 7948-2708, https://orcid.org/0000-0002-5925-4561

Колосов Валерий Николаевич, д.т.н., главный научный сотрудник, Институт химии и технологии редких элементов и минерального сырья им. И.В.Тананаева – обособленное подразделение Федерального государственного бюджетного учреждения науки Федерального исследовательского центра «Кольский научный центр Российской академии наук» (ИХТРЭМС КНЦ РАН) (184209, Россия, г. Апатиты, Мурманская обл., Академгородок, д. 26а). E-mail: v.kolosov@ksc.ru. ResearcherID Q-8446-2017, Scopus Author ID 35275498200, SPIN-код РИНЦ 1801-2839, https://orcid.org/0000-0002-4749-236X

Translated from Russian into English by N. Isaeva
Edited for English language and spelling by Dr. David Mossop